Efficient Raman Sidescatter and Hot-Electron Production in Laser-Plasma Interaction Experiments

R. P. Drake, R. E. Turner, B. F. Lasinski, K. G. Estabrook, E. M. Campbell, C. L. Wang, D. W. Phillion, E. A. Williams, and W. L. Kruer
Lawrence Livermore National Laboratory, Livermore, California 94550
(Received 29 May 1984)

These experiments studied the Raman instability occurring at densities below the quarter-critical density of the incident 0.53-μm laser light. Solid gold targets were irradiated by up to 4 kJ of energy in a 1-ns pulse with focal spots of 150 to 1880 μm. The angular distribution of the Raman scattering shows efficient Raman sidescatter. The energy in electron plasma waves accounts for the hot-electron production over almost three orders of magnitude. We report the results and discuss the implications for laser fusion.

PACS numbers: 52.35.Py, 52.25.Mq, 52.50.Jm

High-intensity laser light can excite parametric instabilities that scatter or absorb it. One instability that can arise when laser light penetrates a plasma is sub-quarter-critical stimulated Raman (SQSR) scattering.[1,2] It occurs below the quarter-critical density of the incident light, and involves the decay of the incident light wave into a scattered light wave and an electron plasma wave. The scattered light wavelength is 1 to 2 times the wavelength of the incident light, depending on the plasma density and temperature. This Letter reports studies of SQSR scattering and hot-electron production in plasmas produced by irradiation of thick gold targets with up to 4 kJ of 0.53-μm light in 1-ns [full width at half maximum (FWHM)] pulses. We first summarize the new results, then present the experiments and the data, and finally discuss the implications for laser fusion.

These are the first observations of intense (up to 0.015 J/J·sr) SQSR sidescatter of submicron laser light, and the first observations of preferential SQSR scattering perpendicular to the plane of the electric vector of the laser beam (out of plane). We attribute this to the combination of large axial density-gradient scale lengths (>100 μm), large irradiation spots (150 to 1880 μm), hot plasmas (>1 keV), and extensive diagnostics. Previous experiments have observed SQSR backscatter[3-6] or have observed SQSR sidescatter that was orders of magnitude less efficient.[7] Other experiments, using 1-μm irradiation, either did not measure the angular distribution[8] or did not determine the scattering mechanism.[9]

Second, the total SQSR yield (up to several percent) is at least three orders of magnitude larger than has been reported from previous experiments using solid targets.[3,6] Efficient SQSR backscatter (but not sidescatter) has been reported from large, low-Z underdense plasmas, deliberately produced to minimize density gradients.[5,7] Third, this is the first report, from experiments with submicron laser light, of a large (up to several percent) yield of suprathermal electrons with a temperature larger than 15 keV. This is important because short-wavelength lasers are being developed to reduce hot-electron production in laser-fusion targets. The only previous report of hot-electron yields this large that were not attributed to resonance absorption was from 1-μm irradiations.[8] Low yields of very-high-energy electrons, attributed to Raman forward scattering, have been reported from 10.6-μm experiments.[10]

Fourth, these are the first experiments in which the total yields of SQSR scattered light, $\frac{3}{2}\omega_0$ light, and hot electrons were simultaneously measured. They included a systematic variation of the irradiation conditions, which allows us to attribute the hot-electron production to SQSR scattering. Thus, they support and complement the previously reported interpretation of results at 10.6 μm[5,11] and 1.06 μm.[8,12] They also are consistent with a model of SQSR scattering and hot-electron production, based on computer simulations of Raman backscatter.[2]

The laser was the Novette laser, at Lawrence Livermore National Laboratory. It produces two opposed, linearly polarized, 74-cm-diam, 0.53-μm beams which are focused onto the target by $f/4$ doublet lenses. Output-sensor modules measure the energy and pulse history of these beams. (The residual intensity of 1.05-μm light at the target plane is about 3×10^{10} W/cm^2.) For most of these experiments, only one beam was fired, and it struck the target while converging toward best focus. The gold targets were at least 1200 μm in diameter and 5 μm thick. X-ray micrographs (at x-ray energies of 1 to 3 keV) determined the focal spot size. The average intensity varied from 10^{14} W/cm^2 to 2×10^{16} W/cm^2. On the basis of the images of the

green beam obtained by the sensor package, the peak-to-average intensity variations at the target plane were no more than 10 to 1 and the intensity over half the area was within a factor of 2 of the average.

An array of filtered, absolutely calibrated photodiodes, sensitive to wavelengths of 0.59 to 1.0 μm and excluding light near 1.05 μm, measured the SQSR scattering from the target. Time-integrated and time-resolved spectra of the Raman emissions verified that the spectrum was characteristic of SQSR. The Raman spectrum peaked near 900 nm, was less than 200 nm wide (FWHM), did not change markedly with irradiation conditions, and lasted for most of the laser pulse. The time-resolved spectra of the sidescatter and the backscatter were both similar to the backscatter spectra reported from a previous experiment.[6]

Figure 1 shows a typical angular distribution of the SQSR light. The measured fluence is shown as joules per steradian times $\sin\theta$ versus the polar angle, θ. Various detectors measured the fluence in plane, out of plane, and in between. The backscatter (defined here as scattering from 148 to 180 deg) showed azimuthal asymmetries of no more than a factor of 2. In contrast, the sidescatter (from 90 to 148 deg) was most often strongly out of plane.

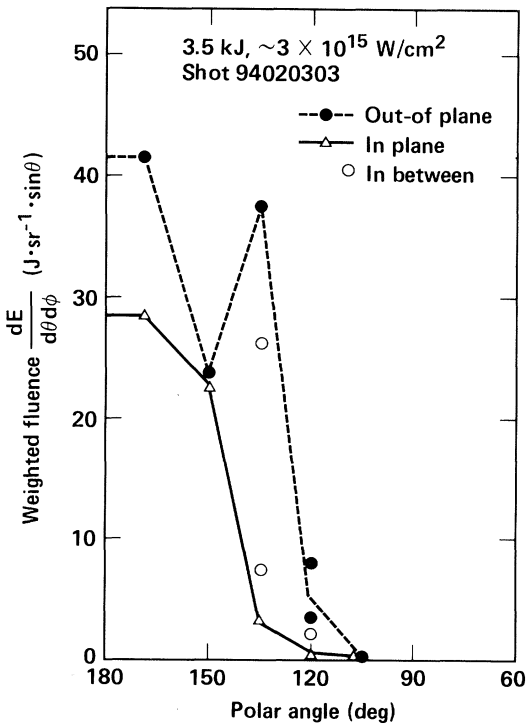

FIG. 1. Angular distribution of Raman-scattered light. See text for details.

The sidescatter was intense (up to 0.015 J/J·sr), and was strongest at a polar angle of 120 to 135 deg. The backscatter was usually a few times more intense than the sidescatter.

We integrated the SQSR fluence over all solid angle to obtain the energy. There are enough detectors that the integrated energy was not strongly sensitive to the model used. For example, the extrapolation to $\theta = 0$ shown in Fig. 1 is not physical, but plausible physical models do not significantly change the integral. A few SQSR measurements, obtained by detectors within the lens cone, support this conclusion. The absorption of the SQSR light by inverse bremsstrahlung is small ($< 10\%$). The absolute uncertainty in the SQSR yield is a factor of 2. The yield inferred from the data in Fig. 1 was 4.4%, with about $\frac{2}{3}$ of the energy as backscatter. This was typical, but the ratio of backscatter to sidescatter varied considerably from shot to shot. The total SQSR yield increased from about 10^{-4} at an average intensity of 10^{14} W/cm^2 to several percent at average intensities above 10^{15} W/cm^2. Comparisons to thresholds are difficult (and are beyond the scope of this paper) because the plasma conditions and the intensity distribution of the beam are not precisely known.

A multichannel, absolutely calibrated x-ray spectrometer used scintillators with photomultiplier tubes to measure the energetic x rays. Some channels used K-edge filters only and others used a prefilter, an x-ray fluorescer, and a post-filter for higher resolution. We used an iterative unfolding procedure that did not constrain the shape of the spectrum[13] to evaluate the x-ray spectra. The absolute magnitude of the x-ray spectrum yields the total energy content of the hot electrons that produced the x rays to within some factor of order 2, as previously described.[14] One source of uncertainty is that some hot electrons may escape the target without producing x rays.

Figure 2 shows a characteristic x-ray spectrum. Each point is plotted at the energy at which that channel has received 50% of its total signal. The x-ray spectra show one or more low-energy components with temperatures below 10 keV, and an exponential decay with a temperature of 20 to 40 keV. This corresponds to a Maxwellian electron distribution of the same temperature. We never detected a more energetic "superhot" component of the spectrum. Any superhot component in the spectrum shown in Fig. 2 contains less than 0.003% of the laser energy (the hot component represents 0.1%).

The SQSR yield and the hot-electron yield

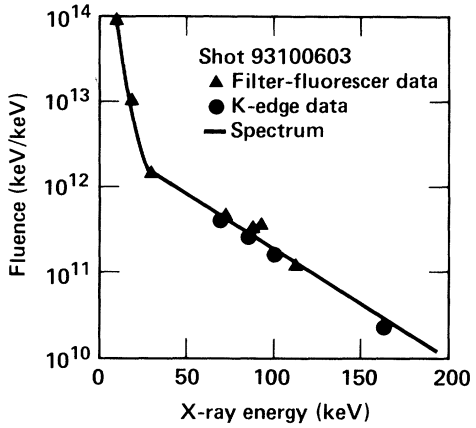

FIG. 2. The hard x-ray spectrum from a Au disk. Irradiation conditions: 3.6 kJ, 1 ns, 740-μm spot.

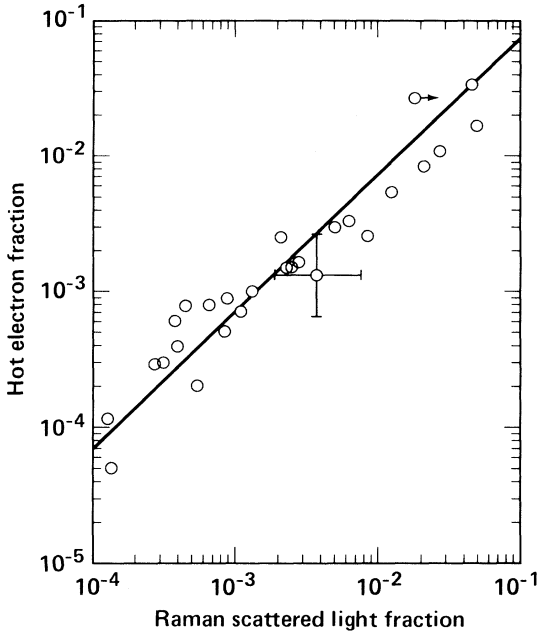

FIG. 3. The hot-electron fraction is well correlated with the Raman light fraction. These quantities are inferred from data like those shown in Figs. 1 and 2.

(f_{HOT}) both increased strongly as the average intensity on target approached 10^{15} W/cm^2. However, both quantities show significant scatter when compared to the average intensity and the observed spot size. They correlate better with one another. The data in Fig. 3 show f_{HOT} as a function of the yield of SQSR light. The line shows the energy in SQSR plasma waves for SQSR scattering at 900 nm (from conservation of energy). Within the uncertainties, f_{HOT} equals the energy in plasma waves as both quantities increase almost three orders of magnitude. Thus, the SQSR yield is sufficient to account for all the hot electrons, although the absolute uncertainties would allow another process of comparable magnitude and similar scaling to contribute. Also, the fact that f_{HOT} and the SQSR yield correlate better with each other than with intensity or spot size strengthens the case that the hot electrons result dominantly from SQSR scattering. In addition, the $\frac{3}{2}\omega_0$ emissions during these experiments correlate less well with intensity or f_{HOT} than the SQSR emissions do. This suggests that instabilities at quarter-critical density are not significant sources of hot electrons in these experiments.

The observed hot-electron temperatures also can be caused by SQSR scattering. When plasma waves undergo Landau damping they produce hot electrons with velocities comparable to the phase velocity of the plasma waves. (In these experiments, the phase velocity of the plasma waves is very insensitive to the thermal electron temperature.) The phase velocities implied by the observed spectra and angular distributions correspond to electron energies of 14–40 keV, which are consistent with the observed temperatures of 20 to about 40 keV. The observed temperatures are not a strong enough function of intensity to result dominantly from resonance absorption.

In conclusion, we consider the implications of these results for laser fusion. The hot electrons produced by the SQSR instability are of concern to laser fusion because they can penetrate and preheat the fusion fuel, making it more difficult to achieve high-gain implosions. This instability may be important in such targets, because it occurs at low densities (and thus is not easily affected by inverse bremsstrahlung) and throughout large volumes of plasma. The data from 10.6-, 1.06-, and 0.53-μm experiments (at low to moderate $I\lambda^2$) indicate that long plasma scale lengths are necessary to produce efficient SQSR scattering from densities below quarter critical. With large plasmas, even solid targets irradiated with submicron light can produce significant scattering and hot-electron production. The SQSR yields could be even larger for the larger plasmas in a laser fusion reactor, especially if the target produces a less collisional low-Z plasma. The important issue for laser fusion is the level at which SQSR scattering will saturate in very large plasmas. Collisional effects may help, by causing the instability to saturate more easily when even shorter-wavelength irradiation is used. Further experiments are needed to see the extent to which Raman scattering limits the intensity and wavelength of the laser light and the collisionality of the plasmas

needed for high-gain systems.

We acknowledge useful discussions with W. C. Mead, T. W. Johnston, and E. McCauley. The experiments would not have been possible without substantial efforts by the Novette scientific and technical staff. The data would not have been analyzed without the extensive contributions of J. Auerbach and B. DeMartini. C. W. Hatcher and the Target Fabrication Program provided the targets. This work was performed under the auspices of the U.S. Department of Energy by Lawrence Livermore National Laboratory under Contract No. W-7405-ENG-48.

[1]C. S. Liu, M. N. Rosenbluth, and R. B. White, Phys. Fluids **17**, 1211 (1974).

[2]K. G. Estabrook, W. L. Kruer, and B. F. Lasinski, Phys. Rev. Lett. **45**, 1399 (1980).

[3]K. Tanaka *et al.*, Phys. Rev. Lett. **48**, 1179 (1982).

[4]R. G. Watt, R. D. Brooks, and Z. A. Pietrzyk, Phys. Rev. Lett. **41**, 170 (1978).

[5]A. A. Offenberger, R. Fedosejevs, W. Tighe, and W. Rozmus, Phys. Rev. Lett. **49**, 371 (1982).

[6]R. E. Turner, D. W. Phillion, E. M. Campbell, and K. G. Estabrook, Phys. Fluids **26**, 579 (1983).

[7]H. Figueroa *et al.*, Phys. Fluids **27**, 1887 (1984).

[8]D. W. Phillion *et al.*, Phys. Fluids **25**, 1434 (1982).

[9]D. W. Phillion *et al.*, Phys. Rev. Lett. **49**, 1405 (1982).

[10]C. Joshi *et al.*, Phys. Rev. Lett. **47**, 1285 (1981).

[11]R. Berger, R. D. Brooks, and Z. A. Pietrzyk, Phys. Fluids **26**, 354 (1983).

[12]K. A. Nugent and B. Luther-Davies, Phys. Rev. Lett. **49**, 1943 (1982).

[13]K. G. Tirsell, H. N. Kornblum, and V. M. Slivinsky, Lawrence Livermore National Laboratory Report No. UCRL-81478, 1979 (unpublished).

[14]W. C. Mead *et al.*, Phys. Fluids **26**, 2316 (1983).